A NET SHORTWAVE RADIATION MODEL

FOR GLACIERIZED BASINS.

D.S. Munro

Department of Geography
University of Toronto
Toronto, Ontario, M5S 1A1

and

G.J. Young

Snow and Ice Division
National Hydrology Research Institute
Environment Canada
Ottawa, Ontario, K1A 0E7

ABSTRACT

The features of a spatial net radiation model are described with specific reference to the Peyto Glacier Basin, Banff National Park, Alberta. The model distributes global radiation estimates according to slope and aspect. Surface reflectance values are incorporated to calculate net shortwave radiation amounts. The scheme is also dynamic in the sense that global radiation responds to cloud cover and the surface reflectance field is sensitive to snowline migration. Model output may be mapped or integrated to provide total amounts of energy used in meltwater production.

INTRODUCTION

Investigations into snow and ice hydrology have become increasingly important, and sophisticated in recent decades. Sophistication has in part resulted from an improved understanding of relationships between surface-atmosphere energy exchanges and the melt process. The results of surface energy balance studies over snow and ice (Munro and Davies, 1976; McKay and Thurtell 1978) suggest that radiant energy transfer could be a dominant factor in meltwater production.

The results of small-scale investigations provide guidance to modelling hydrologically significant energy exchanges in basins. The findings strongly suggest that net longwave radiative loss is of comparable magnitude to gains obtained in the form of turbulent heat exchange, thus leaving net shortwave radiation as the principal energy supplier. Therefore it seems appropriate to begin a basin model with this term.

A crucial feature of a basin model is the ability to map the distribution of net shortwave radiation, and compare it with accumulation and ablation areas. Advances in the mapping of global radiation in relation to topography have been made by others (Garnier and Ohmura, 1968; Williams et al., 1972). However the exercise has not been extended to provide examples of net shortwave radiation distributions.

Modifications to existing global radiation mapping procedures are proposed here to provide a comprehensive net radiation model for hydrological basins. The changes include a

global radiation model for clear and cloudy sky conditions, which requires a minimum of site-based data. Also, patterns of surface reflectance values are incorporated to estimate net shortwave radiation.

MODELLING APPROACH

Global Radiation

Modern approaches to global radiation modelling separate the amount of solar radiation received at the top of the atmosphere into the direct, S, and diffuse, D, components arriving at the ground. The separation is also necessary for mapping purposes.

The direct component for the clear sky case (denoted by a prime) is given by

$$S' = I_o \cos \theta \ [(1-a_{oz}) \ \psi_r - a_w]$$ (1)

in which a_{oz} and a_w are the respective absorptivities of ozone and water vapour, while ψ_r is atmospheric transmissivity after Rayleigh scattering. I_o is the currently accepted value of the solar constant, and θ, the solar zenith angle, is calculated from standard geometrical relationships (Paltridge and Platt, 1976).

The corresponding formula for diffuse radiation is

$$D' = 0.5 \ I_o \cos \theta \ (1-a_{oz})(1-\psi_r)$$ (2)

where multiplication by 0.5 signifies isotropic scattering. Eqs. (1) and (2) also include attenuation by dust, but details have been omitted here to simplify the presentation.

Models of much the same structure have been successfully used for clear sky radiation by others (Monteith, 1962; Atwater and Brown, 1974; Davies, Schertzer and Nunez, 1975). Appropriate formulae relating absorption and transmission coefficients to the path lengths of various attenuators are well documented (Paltridge and Platt, 1976). Aside from modifications for altitude, the approach is easily extended to mountainous terrain.

Less satisfactory results are obtained under cloudy skies, where it is difficult to assign absorptivities and transmissivities in relation to cloud type. Also, a considerable degree of uncertainty is associated with observer estimates of cloud amount, and the extent to which the observations apply to large areas is doubtful. Difficulties increase in the mountains, where cloud patterns can become localized by topographic control.

Sophisticated treatments of the cloudy sky case consider transmission through multiple layers of cloud (Atwater and Brown, 1974; Davies, Nunez and Schertzer, 1975), using data obtained by observers. However some investigators have employed sunshine records as an estimator of cloud amount (Schulze, 1976; Suckling and Hay, 1977). Cloud amount estimates from suncards are used as a basis for the present model, thus treating the sky as though it were affected by a single cloud layer.

Assuming a one level cloud system, the equation for direct radiation becomes

$$S = S' \ (1-n)$$ (3)

in which n is the fractional amount of cloud. A more complex formula applies to the diffuse component:

$$D = D'(1-n) + n \ S'[(1-a_c) \ \beta_c + \alpha_c \ (1-n)(1+\alpha)]$$ (4)

in which a_c is the absorptivity of cloud, β_c a cloud transmissivity, α_c the reflectivity of the cloud base, and α is the surface reflection coefficient. Plausible values for cloud coefficients can be obtained from the literature (Paltridge and Platt, 1976), and modified in light of measured diffuse radiation at the ground. Such an approach is crude but

acceptable in view of the generally small magnitude of the diffuse component.

Estimates from Eqs. (3) and (4) are distributed spatially by incorporating the effects of slope angle and aspect, as described in Kondratyev (1969). Hence the expression for direct radiation on a slope, S_*, is

$$S_* = S \sec \theta \cos i \tag{5}$$

where i is the angle of incidence. The computational procedure for determining i from slope angle and azimuth is described elsewhere (Ohmura, 1968; Williams et al., 1972).

Diffuse radiation on a slope, D_*, can be estimated from

$$D_* = D \cos^2 (Z/2) \tag{6}$$

in which Z is the slope angle. This is essentially a view-factor relationship in which diffuse radiation from other areas visible to the slope is ignored. Thus a slight underestimation of D_* may be expected in glacierized basins, where highly reflective surface elements can be found.

As it is not possible to integrate Eq. (5) over time, daily totals of S_* are obtained from a summation of half-hourly amounts. Previous investigators have found that 30 min. is a suitably small interval of time on which to base summations (Garnier and Ohmura, 1968; Williams et al., 1972). Daily totals of D_* are obtained directly from Eq. (6) and added to the S_* total for the corresponding location to obtain global radiation for the day. The end result includes corrections for shade.

Net Radiation

Net shortwave radiation, K_*, is obtained by applying the surface reflection coefficient to the global radiation:

$$K_* = (S_* + D_*)(1-\alpha) \tag{7}$$

Thus, a net radiation map is obtained from a map of surface reflectivity. In computational terms this means providing a matrix of α values to accompany the matricies of S_* and D_*, as outlined in the computer program of Williams et al. (1972).

Reflectivities vary widely in glacierized basins, from low values (<0.3) over bare rock to relatively high values over snow (>0.8). The range can be large over the glacier surface itself (Hoinkes, 1955). Moreover short-term variations arise from changes in the physical characteristics of snow (Bergen, 1975), and the spectral composition of incident radiation (Holmgren, 1971).

The task of assigning reflectivities, where surface conditions change substantially over time and space, cannot be done with precision. Therefore a simple approach is taken in which the basin is first divided into glacier, and non-glacier areas. Secondly, the recorded position of the snowline defines the upper elevation of ice or firn. It is also possible to classify the snow as new or old, depending upon whether the snowline has advanced or retreated, the latter signifying old snow.

Suitable reflection coefficients are assigned to each surface type from information collected in the field, and placed in the α matrix. The matrix is altered over time as the snowline changes position, thus adding a dynamic aspect to the model by approximating seasonal variations in the basin.

MEASUREMENT ASPECTS

A measurement programme was carried out during July and August of 1978, in the Peyto Glacier Basin, Banff National Park, Alberta; the test area for the net radiation model. The measurements accomplished three objectives:

1) the acquisition of test data to compare with estimated values of global and diffuse radiation,

2) the supply of background data required in the mapping of global radiation, and

3) the documentation of surface reflectance to provide a basis for examining the net shortwave radiation pattern.

Mol-Gorcznski pyranometers (Kipp-Zonen, CM 6) were used to measure global and diffuse radiation at the base camp. The latter was obtained by constructing a shading ring to shield one of the pyranometers from direct radiation. Instrument calibrations were checked prior to, and after the end of the observation period by the Atmospheric Environment Service of Canada.

Radiation data were collected on a strip-chart recorder, from dawn until dusk, on clear and cloudy days. Most of the measurements were obtained under partly cloudy conditions, as there were few occasions when the sky was completely clear or totally overcast.

Measurements of temperature and relative humidity were obtained from a thermo-hygrograph (Lambrecht, No. 252) located on a medial moraine near the equilibrium line of the glacier. They were converted to vapour pressure values, which were substituted into an empirical formula (Kondratyev, 1969) to estimate the path length of water vapour. This was usually found to be approximately 8 mm, a result which is similar to radiosonde estimates obtained for the nearby Marmot Creek Basin (Ferguson et al., 1971). The path length of ozone was assumed to be 3 mm.

The duration of bright sunshine was recorded on suncards mounted in a Campbell-Stokes sunshine recorder (Lambrecht, No. 1604). The fractional duration of sunshine received in half an hour was subtracted from unity to provide an estimate of cloud amount. The estimates were employed, with absorptivities calculated from water vapour and ozone path lengths, in the radiation model.

A portable radiometer stand was constructed for use at various points in the basin. The stand was mounted on a set of gimbals attached to a sled, thus allowing measurements to be made over sloping terrain. Miniature pyranometers, of a black and white design, were mounted on the stand to monitor incoming and outgoing shortwave radiation.

Signals at a given location were continuously monitored on a strip chart recorder. The data were subsequently reduced to provide hourly estimates of the surface reflection coefficient. Thus it became possible to build up an inventory of diurnal reflectivity patterns for a variety of surfaces.

MODEL RESULTS

Global Radiation Predictions

The model seems to provide a good representation of global and diffuse radiation under a clear sky (Fig. 1a). Marked differences occur near sunrise and sunset because the example does not include the effects of shading. These were added later, in the mapping program. Because the global and diffuse results compare closely with measurements, it can be assumed that the direct component is fairly accurate. Thus a global radiation mapping exercise would probably be quite successful under clear skies.

As expected, predictions for a partly cloudy day compare poorly with measurements (Fig. 1b). Although there is fair agreement between measured and predicted global radiation values, the diffuse component is substantially underestimated, thus indicating an erroneously large direct component. This implies that a global radiation map for the day
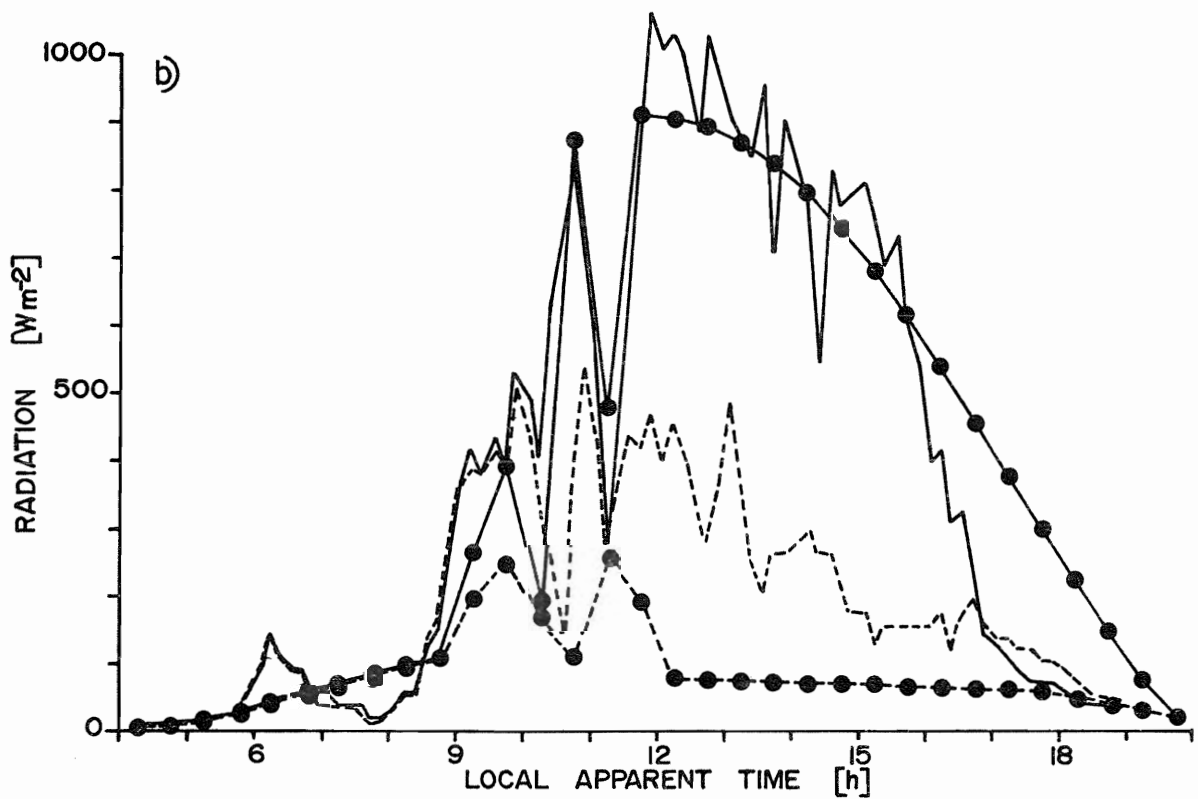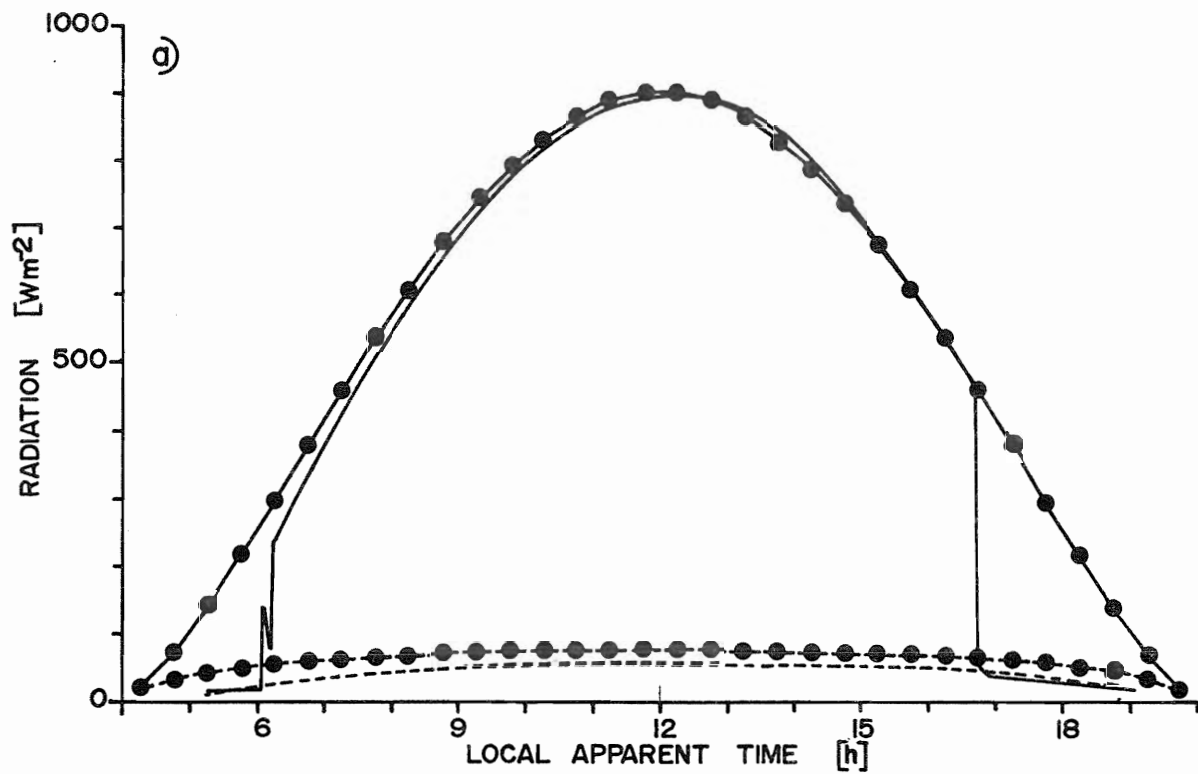
Fig. 1. Comparison of measured and predicted values of global (solid lines) and diffuse (dash lines) radiation for a) August 3, 1978, and b) August 1, 1978. Closed circles denote predicted values.

could convey false impressions due to the different ways in which topography affects the components. In this case one might be wary of enhanced contrasts between shaded and open areas of the basin resulting from an overestimate of direct radiation.

An elevation matrix was extracted from a map of the Peyto Glacier Basin to provide data for slope angle and aspect calculations. The results were applied in Eqs. (5) and (6) to map the distribution of global radiation for various days. Initially, a 100 m separation between points was used. However it was discovered that a 200 m separation provided an adequate map at greatly reduced cost.

Total global radiation amounts were mapped for the partly cloudy sky case (Fig. 2). Considerable spatial variation occurs within the basin. For example, relatively low values are found on east facing slopes in the vicinity of Peyto Peak, Trapper Peak and Mount Baker. The same is true of the north facing slopes of Mount Rhondda and Mount Thompson. Conversely, relatively high values ($\geq$ 22.5 MJ day^{-1}) appear on south facing slopes.

Low values on north facing slopes may be interpreted as a consequence of steep angles and shading. Similar reasoning can be invoked for east facing slopes, though the additional factor of cloud distribution must be considered. Suppressed east slope values are in part due to a reduction of direct radiation by cloud in the morning (Fig. 1b), a time when east slopes receive the greatest amount of radiation.

Small angles of incidence account for large radiation income on south facing slopes. These are also favoured by a westward component to their orientation, because direct radiation is strongest in the afternoon (Fig. 1b). The interpretation may be treated cautiously in view of the shortcomings noted in the radiation model for cloudy days.

Topographic variations in global radiation are not the most notable feature of the glacier surface itself, except near the continental divide, where shading effects are important. Glacier surface variations are more strongly expressed in the distribution of net shortwave radiation.

Net Shortwave Radiation

Diurnal patterns of reflection coefficients were documented for a variety of surface conditions. In some cases the values appeared to be smaller toward local noon, an indication of dependence upon the angle of incidence. Nevertheless, the dependence did not seem sufficiently strong to warrant modelling. Consequently daily mean values were used to characterize surface conditions.

The reflectivities were grouped into broad classes of surface type, and class averages were obtained. Thus a classification into new snow, old snow, firn, exposed ice and rock established respective values of 0.74, 0.61, 0.50, 0.25 and 0.24 for the reflection coefficients. These were assigned according to the rules of the model, taking the value for rock outside the area of the glacier. A firn value was assigned to areas between the snow-line and the equilibrium line of the glacier, when the snowline had migrated above the elevation of the equilibrium line.

Mapping was confined to the glacierized areas of the basin (Fig. 3). Because of the large difference between ice and old snow reflectivities, the snowline is a striking feature of the net radiation map, marked by the proximity of the 12.5 and 15 MJ day^{-1} isolines. It clearly separates the lower and upper areas of the glacier into different energy regimes.

The net radiation model is at best an approximation of the real case. However it provides a useful illustration of the effect which snowline migration could have upon the energy regime of the basin. The glacier is thus characterized as a large solar collector in which the position of the snowline determines the absorptivity. This, in turn, influences discharge from the basin.
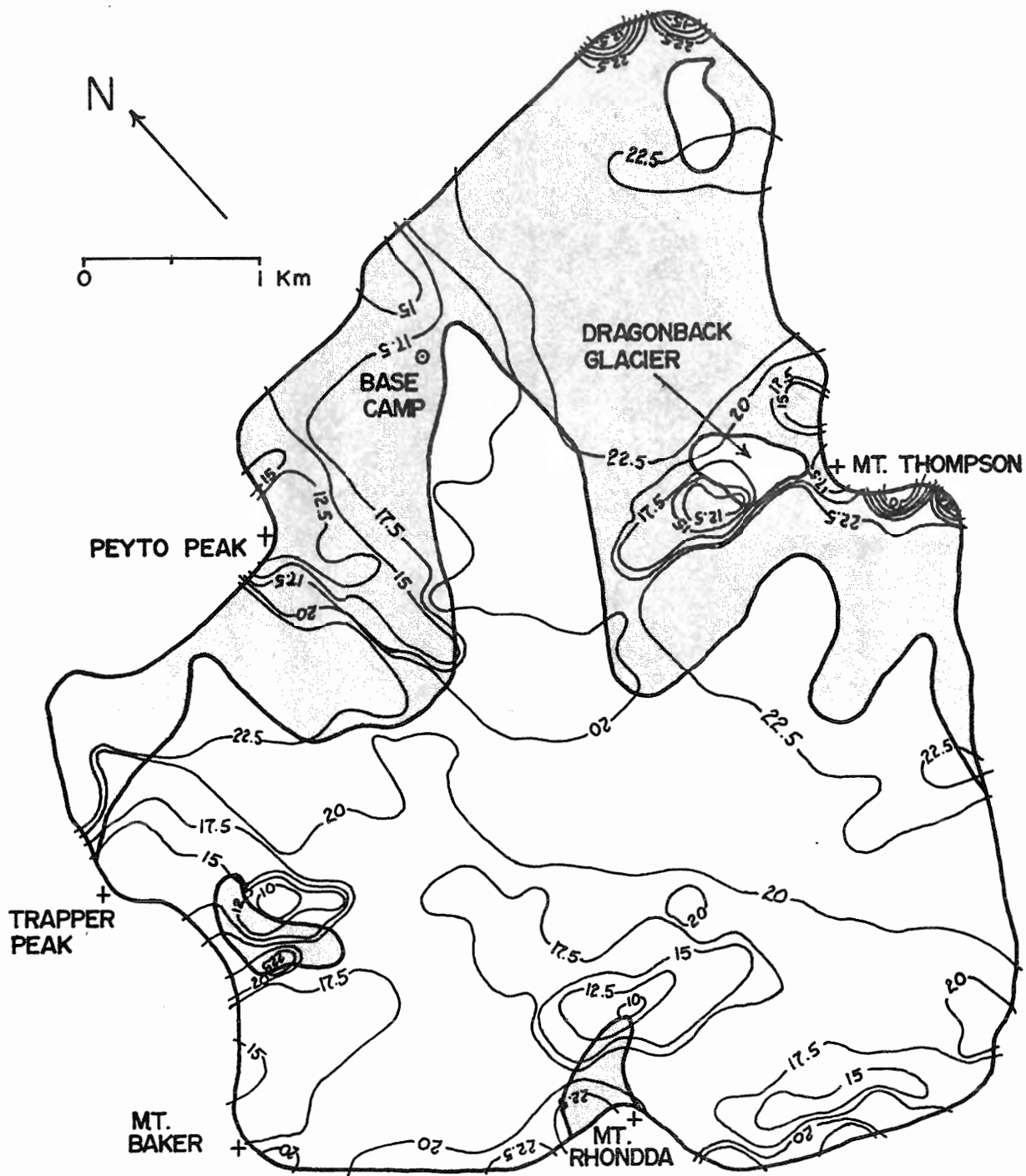
Fig. 2. Distribution of global radiation in the Peyto Glacier Basin, August 1, 1978. Values are in MJ day^{-1}. Non-glacerized areas are shaded.
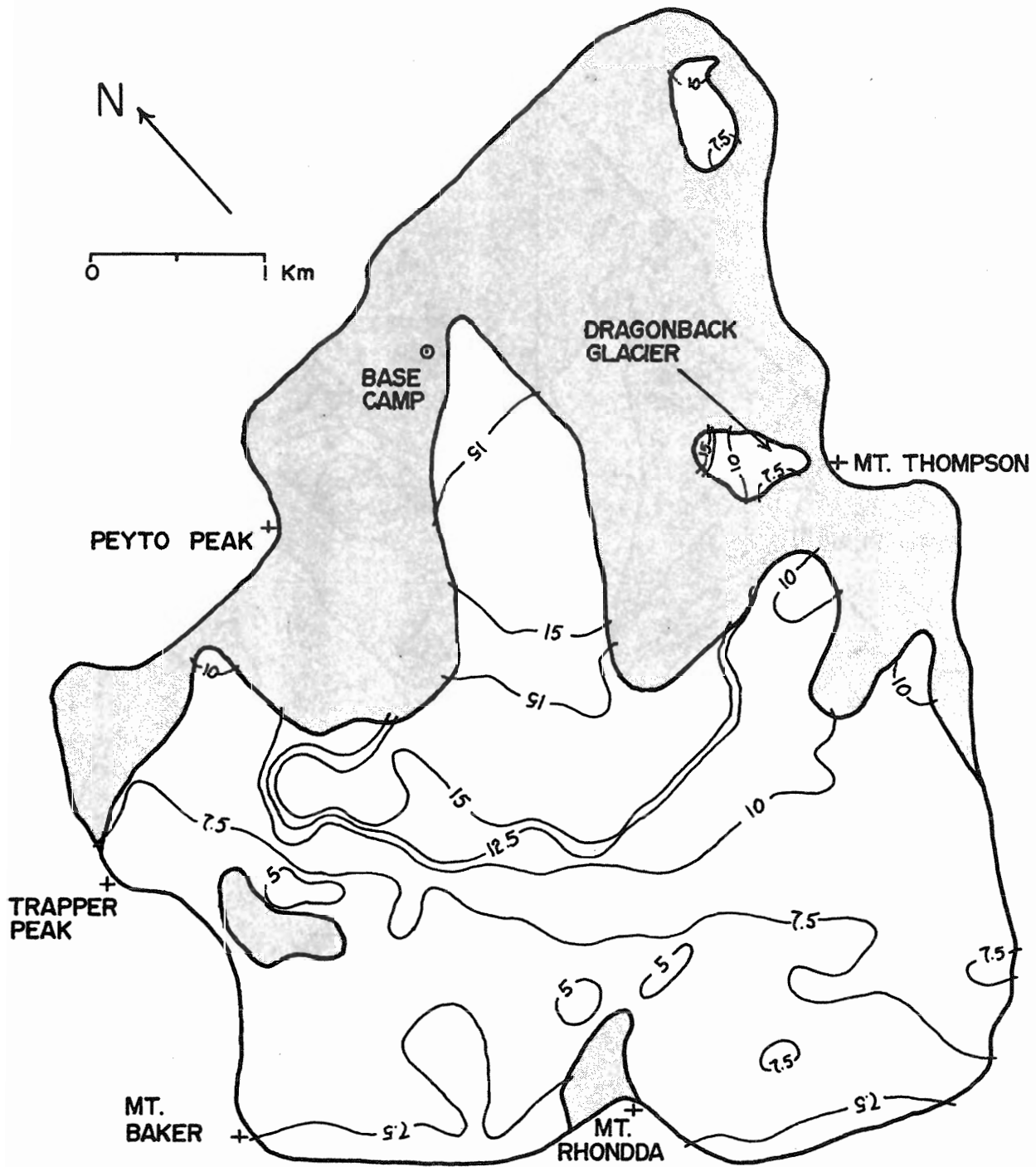
Fig. 3. Distribution of net shortwave radiation on the glacier surface, August 1, 1978. Notation as in Fig. 2.

DISCUSSION

Due to its northerly aspect, and topographic shading, the glacier surface is exposed to slightly more than 90% of the global radiation available on a horizontal plane. Approximately half of this amount is absorbed as net shortwave radiation in the example provided here (Fig. 3). However, the main utility of the model is to characterize energy receipt in different zones of the glacier. This is conveniently done by examining the altitudinal distribution of radiation (Fig. 4).

A comparison of global radiation received in the accumulation zone with the basin average indicates that it receives less energy than its surroundings (Fig. 4a). This is a consequence of the generally southern aspect of non-glacierized areas, and the northerly orientation of snow and ice covered areas in the upper zones of the basin. On the other hand, the ablation zone tends to be energetically similar to its surroundings.

If such a comparison is applicable over a long time period, it might be used to interpret the mass balance. For instance, it could be argued that topographic effects tend to preserve the accumulation area by reducing the amount of energy available for melting snow. This, however, ignores a different aspect of topography, the extent to which it controls the distribution of snow accumulated during the winter.

The contrast between the accumulation area, and its surroundings is enhanced in the plot of net shortwave radiation (Fig. 4b) because different reflection coefficients apply to the two areas. Again, the ablation area below the snowline is energetically similar to its surroundings because the reflectivity of glacier ice is virtually the same as that of rock.

The significance of snowline migration in the ablation zone is seen in the contrasting net shortwave radiation values between 2500 and 2700 m (Fig. 4b). The effects are less important in the accumulation zone because firn has a relatively high reflectivity. In the context of the entire glacier system, the maximum elevation attained by the snowline during a particular summer signifies an energy regime which may change the position of the equilibrium line.

CONCLUSION

The details of a net shortwave radiation mapping model have been outlined. The model can be applied with the aid of a topographic map and a limited data base. Although some components of the model only roughly approximate real conditions, it is a potentially useful tool in the investigation of mass balance relationships, and glacier hydrology.

Important innovations are global radiation predictions for cloudy as well as clear sky conditions, and sensitivity to the changing character of the surface. These are at an early stage of development, and refinments will likely be sought. However the general structure of the model appears to be sound. Therefore, it provides an appropriate framework for the investigation of hydrologically significant energy exchanges in glacierized basins.
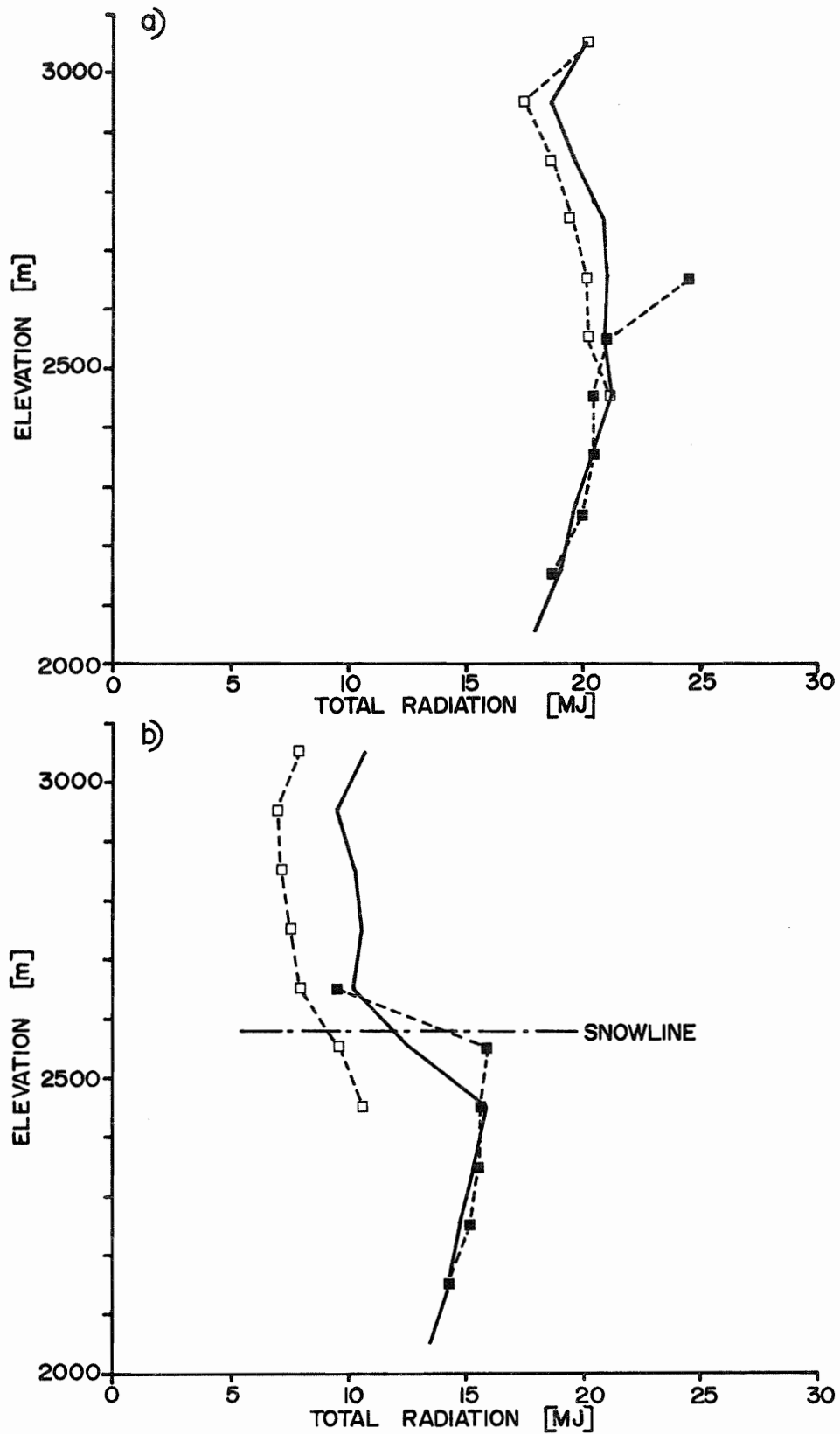
ACKNOWLEDGEMENTS

Fig. 4. Altitudinal distribution of a) global radiation, and b) net shortwave radiation on the glacier surface (dash lines) compared with basin averages (solid lines) for August 1, 1978. Open squares denote the accumulation zone, solid squares the ablation zone.

REFERENCES

Atwater, M.A., and P.S. Brown, 1974: Numerical computations of the latitudinal variation of solar radiation for an atmosphere of varying opacity. J. Appl. Meteorol. 13, 289-297.

Bergen, J.D., 1975: A possible relation of albedo to the density and grain size of natural snow cover. Water Resour. Res., 11, 745-746.

Davies, J.A., W. Schertzer, and M. Nunez, 1975: Estimating global solar radiation. Boundary-Layer Meteorol., 9, 33-52.

Ferguson, H.L., H.F. Cork, R.L. Anderson, S. Matoris, and B. Weisman, 1971: Theoretical clear-sky effective insolation over a small mountain basin. Climatol. Studies, 21, Toronto, Atmospheric Environment Service, 45 pp.

Garnier, B.J., and A. Ohmura, 1968: A method of calculating the direct shortwave radiation income of slopes. J. Appl. Meteorol., 7, 796-800.

Hoinkes, H., 1955: Measurements of ablation and heat balance on alpine glaciers, J. Glaciol., 2, 497-501.

Holmgren, B., 1971: Climate and energy exchange on a sub-polar ice cap in summer. Part E. Radiation climate. Meddelande, Nr 111, Uppsala, Meteorologiska Institutionen Uppsala Universitet, 111 pp.

Kondratyev, K. Ya., 1969: Radiation in the Atmosphere. New York, Academic Press, 485-502.

McKay, D.C., and G.W. Thurtell, 1978: Measurement of the energy fluxes involved in the energy budget of a snow cover. J. Appl. Meteorol., 17, 339-349.

Monteith, J.L., 1962: Attenuation of solar radiation: a climatological study. Quart. J. Roy. Meteorol. Soc., 88, 508-521.

Munro, D.S. and J.A. Davies, 1978: Diurnal energy flux variations and glacier surface hydrology, pp. 75-77 in International Geography 76, (Proceedings of the 23rd International Geographical Congress, Moscow), I.P. Gerasimov, ed., Vol. 2, Oxford, Pergamon Press, 385 pp.

Ohmura, A., 1968: The computation of direct insolation on a slope. Climatol. Bull. (McGill University), No. 3, 42-53.

Paltridge, G.W., and C.M.R. Platt, 1976: Radiative Processes in Meteorology and Climatology. Amsterdam, Elsevier, 318 pp.

Schulze, R.E., 1976: A physically based method of estimating solar radiation from suncards. Agric. Meteorol., 16, 85-101.

Suckling, P.W., and J.E. Hay, 1977: A cloud layer-sunshine model for estimating direct, diffuse and total solar radiation. Atmosphere, 15, 194-207.

Williams, L.D., R.G. Barry, and J.T. Andrews, 1972: Application of computed global radiation for areas of high relief. J. Appl. Meteorol., 11, 526-533.